2D active liner experimental results in acoustic flow duct facility

Kevin Billon, Manuel Collet, Edouard Salze, M Gillet, M Ouisse, M Volery, H Lissek, J Mardjono

2D active liner experimental results in acoustic flow duct facility

K. Billon[a], M. Collet[a], E. Salze[b], M. Gillet[c], M. Ouisse[c], M. Volery[d], H. Lissek[d], and J. Mardjono[e]

[a]Univ. Lyon, École Centrale de Lyon, LTDS UMR 5513, F-69134 Ecully, France
[b]Univ. Lyon, École Centrale de Lyon, LMFA UMR 5509, F-69134 Ecully, France
[c]Univ. Bourgogne Franche-Comté, FEMTO-ST Institute, CNRS/UFC/ENSMM/UTBM, Department of Applied Mechanics, 24 rue de l'Epitaphe, F-25000 Besançon, France
[d]Signal Processing Laboratory LTS2, Ecole Polytechnique Fédérale de Lausanne, Station 11, CH-1015 Lausanne, Switzerland
[e]Safran Aircraft Engines, F-75015, Paris, France

ABSTRACT

This paper is focused on experimental characterization of new active liners technologies in acoustic flow duct facilities (FDF). These measurements have been performed in the NLR (Netherlands Aerospace Center). Different configurations of passive and active treatments have been tested using the same grazing flow conditions (Mach 0.3) in an aeroacoustic test bench: 1 conventional liner (standard SDOF sandwich panels with honeycomb core) used as reference and a 2D active liner based on an array of electroacoustic absorbers. The grazing flow test campaign comprises acoustics and aerodynamics measurements to characterize the aeroacoustics flow conditions, the membrane behavior, the acoustic impedance and the resulting insertion loss.

INTRODUCTION

The SALUTE (Smart Acoustic Lining for Ultra High By Pass Ratio (UHBR) Technologies Engines) project aims at evaluating performance of metacomposites liners for acoustic smart lining in grazing turbulent flow. Theoretical and numerical investigations are carried out for designing innovative specimen. A specific focus is placed in the realization of prototypes for evaluating the metacomposite liner performances in 2D and 3D liners, its process complexity and robustness. The insight gain in this project is new tools for obtaining innovative samples; the acoustical experimental tests demonstrate efficiency and robustness of such technology for controlling UHBR noise emission.

Active Liners can outperform conventional acoustic treatments (Single Degree of Freedom (SDOF) liner for example) and adapt their performances in real-time to varying engine speeds with an external source of energy. The proposed active Noise Control (ANC) strategy is based on an electro-mechano-acoustical system. The pioneers works on the topic[1] introduced an "electronic sound absorbers" with a loudspeaker and a nearby microphone in a negative feedback loop. A few decades later, an "active equivalent of a quarter wavelength resonator" was achieved through a hybrid passive-active technique.[2] This strategy was retrieved by[3] for liners applications.

Recently, the concept of electroacoustic absorber evolved with shunting techniques,[4,5] direct feedback,[6,7] or a sensorless control of the loudspeaker impedance.[8] This pressure-based current-drive control architecture has been applied to design an active lining concept built an arrangement of electroacoustic absorbers. This concept allowed to achieve broadband noise reduction for aircraft engine nacelles applications under grazing flow.[9]

This paper presents an acoustic characterisation of a 2D active liner based on an array of electroacoustic absorbers. The control law is based on the pressure-based, current driven digital architecture for impedance

Further author information: (Send correspondence to Manuel Collet)
E-mail: manuel.collet@ec-lyon.fr

control designed by Rivet et al.[10] A local control strategy[11] is experimentally validated with flow. This paper is organised as follow: the wind tunnel test bench facilty is presented, then, the acoustic liner panels are described with the associated results in terms of acoustic performance.

WIND TUNNEL TEST BENCH FACILITY

The insertion loss measurements are performed in the NLR FDF. The facility is a closed circuit wind tunnel with a test section of $150 \times 300\ mm^2$. For the outlet liner insertion loss measurements Mach numbers up to 0.6 are feasible in this facility. The panels are installed at the sidewalls of the test section and the test section is closed off with the (yellow) steel doors to prevent air and sound leakage near the test section, as shown in Figure 1

The FDF test section is terminated by two 50 m^3 reverberation rooms, see Figure 2. The sound sources are placed in the upstream reverberation room, simulating the outlet liner configuration. Microphone 1 is installed in the upstream reverberation room and microphone 2 in the downstream reverberation room.

The acoustic measurements were performed with a sampling frequency of 40.96 kHz and the block-size was set to 2048, giving a frequency resolution of 20 Hz. The measurement time was 64 seconds. The time signals were recorded by a GBM-Viper data acquisition system, where they passed a high-pass filter (cut-off frequency 1.5 Hz) and an anti-aliasing filter (cut-off frequency approximately 35% of the sampling frequency). After Fourier transformation, the SPL were calculated and averaged. A Hanning window was applied with an overlap of 50%. The Transmission Loss (TL) and Insertion Loss (IL) data were calculated from the SPL data. For each measurement and frequency band, the squared amplitude of the Fourier transformed sound pressure p^2, is calculated from the measured sound pressure level SPL:

Figure 1. FDF test section.

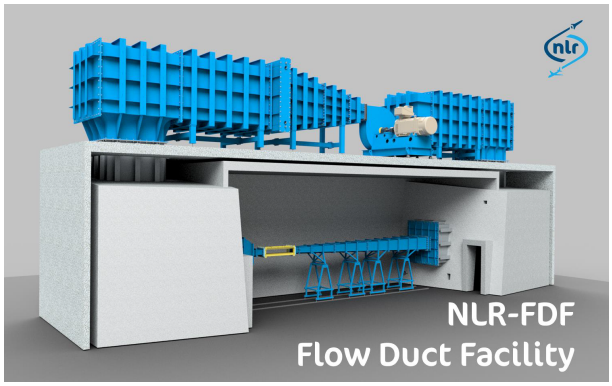

Figure 2. Insertion loss set-up.[12]

$$p^2 = p_{ref}^2 \times 10^{SPL/10} \tag{1}$$

with $p_{ref} = 20\mu Pa$ the reference sound pressure.

The measured sound power levels in the sending and receiving room (p_{sm} and p_{rm}) are corrected for the tunnel background noise (p_{s0} and p_{r0}):

$$p_s^2 = p_{sm}^2 - p_{s0}^2 \tag{2}$$

$$p_r^2 = p_{rm}^2 - p_{r0}^2 \tag{3}$$

The transmission loss values TL_H and TL_L for a hard and a lined wall respectively and the insertion loss IL are then calculated from:

$$TL_H = 10\log_{10}\left(\frac{p_{Hs}^2}{p_{Hr}^2}\right) \tag{4}$$

$$TL_L = 10\log_{10}\left(\frac{p_{Ls}^2}{p_{Lr}^2}\right) \tag{5}$$

$$IL = TL_L - TL_H \tag{6}$$

with the subscripts H and L denoting the hard and lined wall, and the subscripts s and r the sending and receiving room respectively.

ACOUSTIC LINER PANELS

Different liners, lengths and flow configurations have been tested. In this paper, a configuration is highlighted. The counter flow is considered with a flow speed of Mach 0.3. For the insertion loss measurements 2 different liner panels where evaluated. A passive liner used as the reference and an active liner are described below:

- - Liner 540A : Passive reference liner with a length of 540 mm (conventional SDOF sandwich panels with honeycomb core),
- - Liner 800 : Active liner with a length of 800 mm.

Active liner

The active liner is composed of 39 cells (3 lines of 13 cells) covered by a wiremesh to avoid turbulences in front of the microphones and protect the cells with flow. Each active cell is similar to the cells used for the previous experimental campaign[11] which the control law is implemented by pressure-based, current-driven digital architecture for impedance control. In the facility duct, the active liner is mounted with a rigid wall or the passive liner (540A) in front of (Figure 3). The acoustic sealing is ensured by a bell (Figure 4), USB wire for the computer and power supplies wires exit through a sealed instrumentation hole.

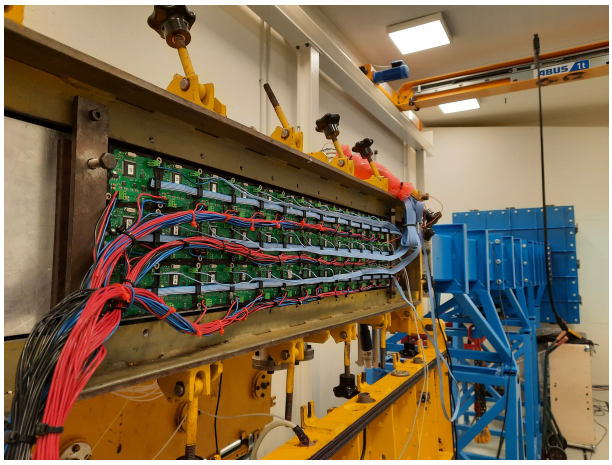

Figure 3. Active liner installed in its dedicated location.

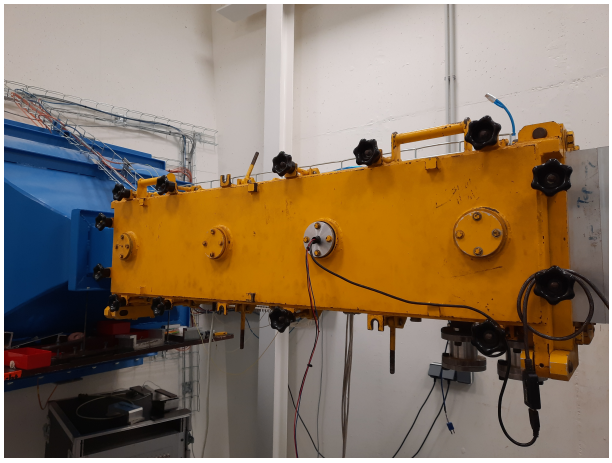

Figure 4. Sealing bell of the test bench.

RESULTS

The passive liner (540A) has been tested. In this configuration, a full hard wall configuration was used as reference. The calculated IL is the effective insertion loss due to the passive liner. The efficiency zone is located around the resonance frequency of the conventional SDOF sandwich panels with honeycomb core (500 Hz). The flow speed is $M0.3$.

In order to put forward the main tendencies of the acoustic properties of the different acoustic liners, different indicators are computed on the frequency band of interest from 300 to 2000 Hz:

- - 1: maximal value of the insertion loss (IL_{max}),
- - 2: frequency at which the insertion loss is maximum ($freq_{IL_{max}}$),
- - 3: average insertion loss on the frequency range of interest (IL_{mean}),
- - 4: mean value taken by the insertion loss when it is greater than 3 dB (IL_{mean} $(IL > 3dB)$),
- - 5: width of the frequency range where the insertion loss when it is greater than 3 dB (Δ_{freq} $(IL > 3dB)$).

Figure 5 shows the performances of the passive liner which is efficient around 500 Hz with an attenuation of 15.4 dB. Indicators corresponding to the Figure 5 are summarized in the first line of the Tables 2 and 3.

The active liner has been tested and compared, in the following, with the passive configuration. The local control strategy has been used identical in its implementation to that previously defined in the article.[11] The efficiency zone is located around the resonance frequency of the locally controlled loudspeaker. This frequency is defined as:

$$f_{eff} = f_0 \sqrt{\frac{\mu_2}{\mu_1}}. \tag{7}$$

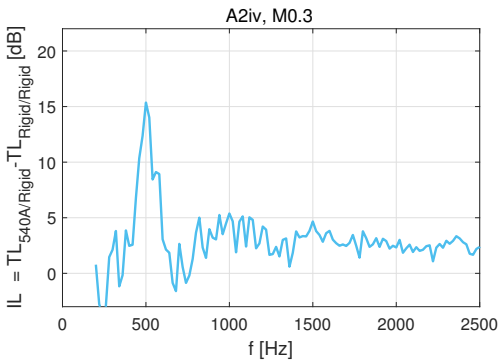

Figure 5. Passive reference liner, flow speed $M0.3$: Insertion loss ($IL = TL_{540A/Rigid} - TL_{Rigid/Rigid}$).

μ_1	μ_2	f_{eff}
0.7	0.26	400 Hz
0.7	0.5	550 Hz
0.7	0.7	$mean(f_0) = 660$ Hz
0.7	1.03	800 Hz
0.7	1.3	900 Hz
0.7	1.61	1000 Hz

Table 1. Efficient frequencies (f_{eff}) depending on the parameters μ_1 and μ_2.

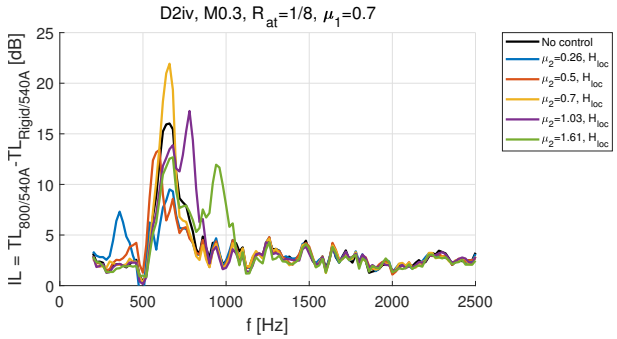

Figure 6. Active liner, flow speed $M0.3$. Effect of the variation of the μ_2 parameters of the control law ($\mu_1 = 0.7$, target resistance $R_{at} = 1/8\rho_0 c_0$) : Insertion loss ($IL = TL_{800/540A} - TL_{Rigid/540A}$).

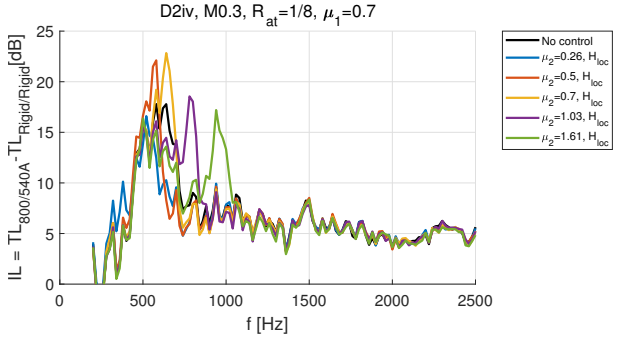

Figure 7. Active liner, flow speed $M0.3$. Effect of the variation of the μ_2 parameters of the control law ($\mu_1 = 0.7$, target resistance $R_{at} = 1/8\rho_0 c_0$) : Insertion loss ($IL = TL_{800/540A} - TL_{Rigid/Rigid}$).

Frequencies where the control is efficient depending on the parameters μ_1 and μ_2 are given in table 1. When these two parameters are equal, the control is efficient around the natural frequency of the loudspeaker (f_0). The minimum value of the μ_1 parameter of the local control law ensuring the stability of the system is equal to 0.7. The μ_1 parameter is constant as it is fixed by high frequency stability constraints, therefore the μ_2 parameter is used to tune the frequency f_{eff} where the control is efficient.

As a reminder, for the active liner, performance is measured with the passive liner at the opposite wall. For these measurements a hard wall and the passive liner configuration was used as reference. The calculated IL for these measurements is therefore only the effective insertion loss due to the active liner.

In this part, the results for the configuration of this paper are presented. Figure 6 shows the performances of the control when the parameters of the control law are varied. The μ_1 parameter of the local control law is 0.7 and μ_2 is changed 0.26, 0.5, 0.7, 1.03, 1.61. The targeted impedance has been selected as $R_{at} = 1/8\rho_0 c_0$, optimal IL values were probably not measured, since only one target resistance was tested. The flow speed is $M0.3$.

For information, results can be given with a full hard wall configuration as reference. The calculated IL for these measurements is the effective insertion loss due to the active liner and the passive liner (Figure 7). The effect of the passive and the active liners are highlighted with absorption at 500 Hz and absorption at f_{eff} depending on the μ_2 parameter. This plot is less relevant to quantify both effects.

Indicators corresponding to the Figure 6 are summarized in the Tables 2 and 3. The reference values for the passive liner configuration is given in the first line of the tables. The other lines are dedicated to the active liner (the second line corresponds to the non controlled configuration). Tables are used to compare the performance of the active liner with the local control for different values of μ_2 parameter and the passive liner.

Unlike the passive liner, the efficiency zone can be adapted according to the frequency with the active liner with better performance around the frequency of the loudspeaker. By moving away from the natural frequency

	IL_{max} $[dB]$	$freq_{IL_{max}}$ $[Hz]$	IL_{mean} $[dB]$
Passive liner	15.36	500	3.5
No control	16.02	660.1	4.0
$\mu_2 = 0.26,\ H_{loc}$	9.51	660.1	3.6
$\mu_2 = 0.50,\ H_{loc}$	13.42	600.1	3.7
$\mu_2 = 0.70,\ H_{loc}$	21.93	660.1	4.0
$\mu_2 = 1.03,\ H_{loc}$	17.26	780.1	4.2
$\mu_2 = 1.61,\ H_{loc}$	12.68	680.1	4.1

Table 2. Indicators (1, 2, 3) for the passive liner (first line) and the active liner (flow speed $M0.3$).

	$IL_{mean_{(IL>3dB)}}$ $[dB]$	$\Delta_{freq_{(IL>3dB)}}$ $[Hz]$
Passive liner	8.9	489
No control	7.3	508
$\mu_2 = 0.26,\ H_{loc}$	5.1	642
$\mu_2 = 0.50,\ H_{loc}$	6.2	482
$\mu_2 = 0.70,\ H_{loc}$	8.5	426
$\mu_2 = 1.03,\ H_{loc}$	8.3	518
$\mu_2 = 1.61,\ H_{loc}$	8.1	532

Table 3. Indicators (4, 5) for the passive liner (first line) and the active liner (flow speed $M0.3$).

of the loudspeaker, the performances remain correct and provide adaptability of the active liner. The results confirm the adaptability and the stability of the whole system with the local control strategy between 400 and 1000 Hz with M0.3 flow velocity.

CONCLUSION

In this section, the acoustic characterisation of the active liner (a 2D active liner based on an array of electroacoustic absorbers) is presented. The control law is implemented by pressure-based, current-driven digital architecture for impedance control (similar that control implementation in the previous experimental campaign[11]). Local control strategy is experimentally validated with air flow on the NLR wind tunnel test rig. Frequencies where the control is efficient depending on the parameters μ_1 and μ_2 of the control law. The minimum value of the μ_1 parameter of the local and non-local control law ensuring the stability of the system is equal to 0.7. The number of cells (39) and the width of the duct make it more difficult to adjust the stability of the whole active liner. The adaptability and the stability of the system between 400 and 1000 Hz with the tested parameters of local control law have been validated. Different indicators are computed (maximum and average insertion loss on the frequency band of interest, frequency at which the insertion loss is maximum, average insertion loss and width of the frequency rang when it is greater than 3 dB) to compare the configurations.

ACKNOWLEDGMENTS

The SALUTE project has received funding from the Clean Sky 2 Joint Undertaking under the European Union's Horizon 2020 research and innovation programme under grant agreement N° 821093. The authors want to thank the NLR team for this experimental test campaign.

REFERENCES

[1] H. F. Olson and E. G. May, "Electronic sound absorber," The Journal of the Acoustical Society of America **25**(6), pp. 1130–1136, 1953.

[2] D. Guicking and E. Lorenz, "An active sound absorber with porous plate," 1984.

[3] M. Furstoss, D. Thenail, and M.-A. Galland, "Surface impedance control for sound absorption: direct and hybrid passive/active strategies," Journal of sound and vibration **203**(2), pp. 219–236, 1997.

[4] H. Lissek, "Shunt loudspeaker technique for use as acoustic liner," in Proceedings of the Internoise 2009: Innovations in Practical Noise Control, pp. 1–8, 2009.

[5] R. Boulandet and H. Lissek, "Optimization of electroacoustic absorbers by means of designed experiments," Applied acoustics **71**(9), pp. 830–842, 2010.

[6] H. Lissek, R. Boulandet, and R. Fleury, "Electroacoustic absorbers: bridging the gap between shunt loudspeakers and active sound absorption," The Journal of the Acoustical Society of America **129**(5), pp. 2968–2978, 2011.

[7] R. Boulandet and H. Lissek, "Toward broadband electroacoustic resonators through optimized feedback control strategies," Journal of Sound and Vibration **333**(20), pp. 4810–4825, 2014.

[8] R. Boulandet, E. Rivet, and H. Lissek, "Sensorless electroacoustic absorbers through synthesized impedance control for damping low-frequency modes in cavities," Acta Acustica united with Acustica **102**(4), pp. 696–704, 2016.

[9] R. Boulandet, H. Lissek, S. Karkar, M. Collet, G. Matten, M. Ouisse, and M. Versaevel, "Duct modes damping through an adjustable electroacoustic liner under grazing incidence," Journal of Sound and Vibration **426**, pp. 19–33, 2018.

[10] E. Rivet, S. Karkar, and H. Lissek, "Broadband low-frequency electroacoustic absorbers through hybrid sensor-/shunt-based impedance control," IEEE Transactions on Control Systems Technology **25**(1), pp. 63–72, 2016.

[11] K. Billon, E. D. Bono, M. Perez, E. Salze, G. Matten, M. Gillet, M. Ouisse, M. Volery, H. Lissek, J. Mardjono, and M. Collet, "In flow acoustic characterisation of a 2d active liner with local and non local strategies.," Applied Acoustics **191**, p. 108655, 2022.

[12] "www.nlr.org,"